

Supporting Information

UbMES and UbFluor: Novel Probes For RBR E3 Ubiquitin Ligase PARKIN

Sungjin Park¹, Peter K. Foote², David T. Krist², Sarah E. Rice¹, Alexander V. Statsyuk,^{2,3}

¹Department of Cell and Molecular Biology, Northwestern University, 303 East Chicago Avenue, Chicago, IL 60611, USA; ²Chemistry of Life Processes Institute, Department of Chemistry, Northwestern University, Silverman Hall, 2145 Sheridan Road, Evanston, Illinois 60208, United States; ³Department of Pharmacological and Pharmaceutical Sciences, College of Pharmacy, University of Houston, 3455 Cullen Blvd., Houston, TX 77204-5037.

1. Synthesis of the Fluorescein thiol (Fluor-SH)

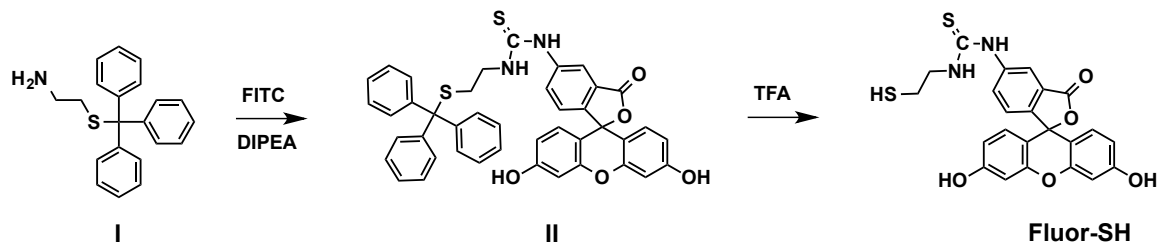
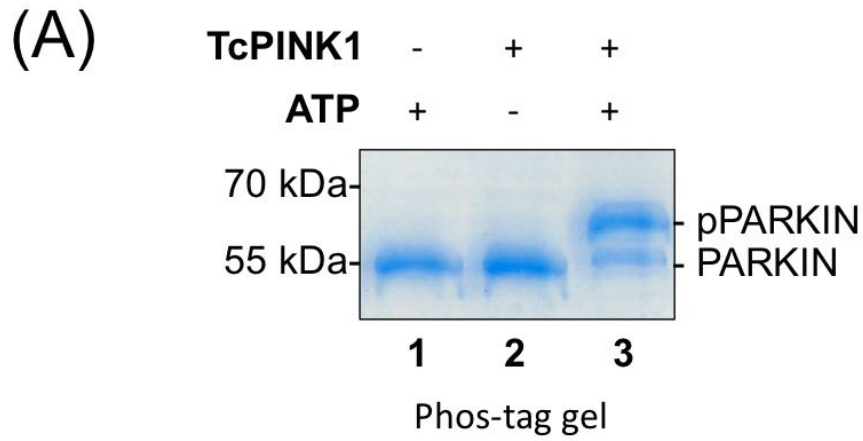


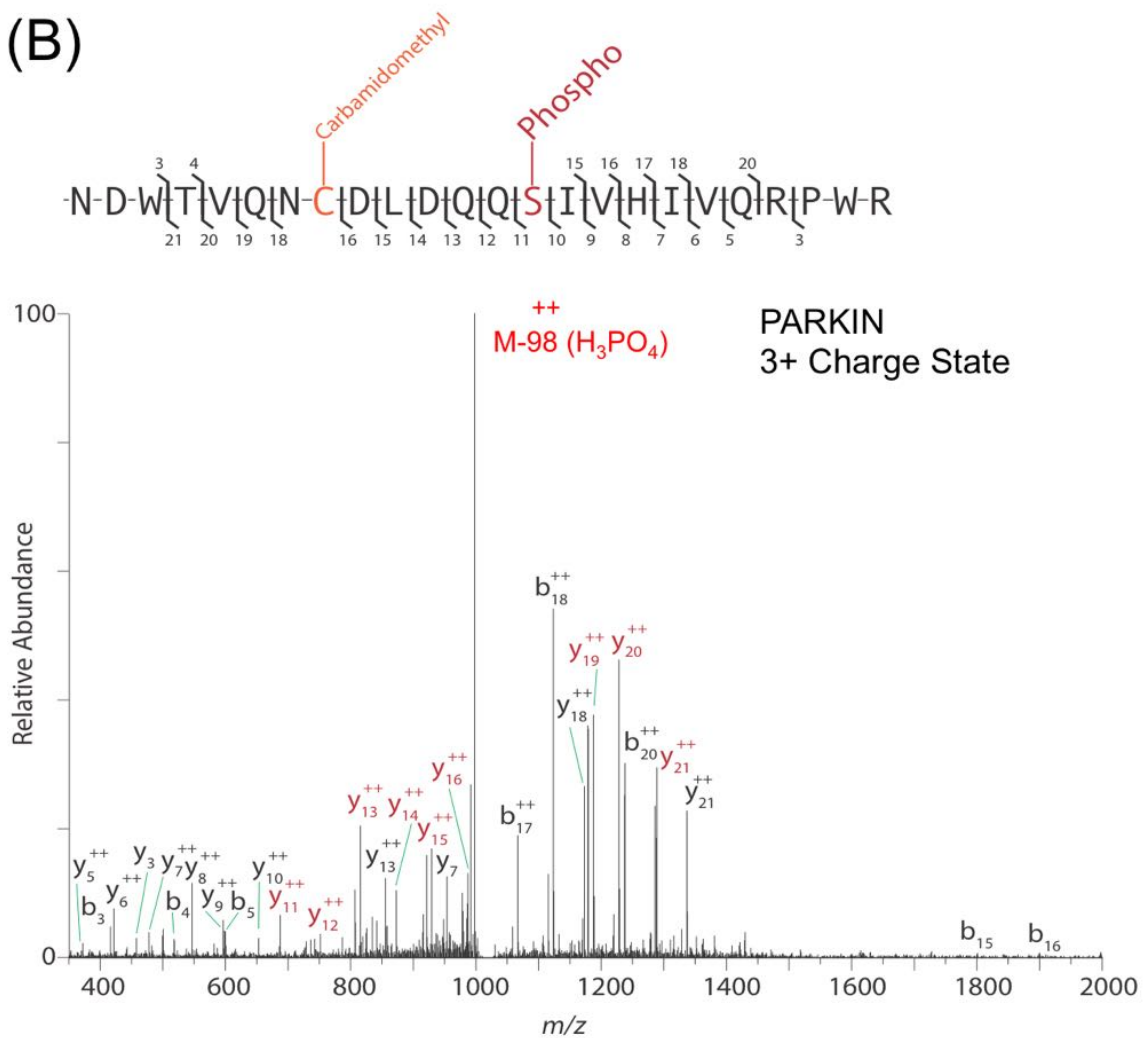
Table S1

	Before reaction started (mP)	After reaction completed (mP)
ST	150	30
MT	135	30

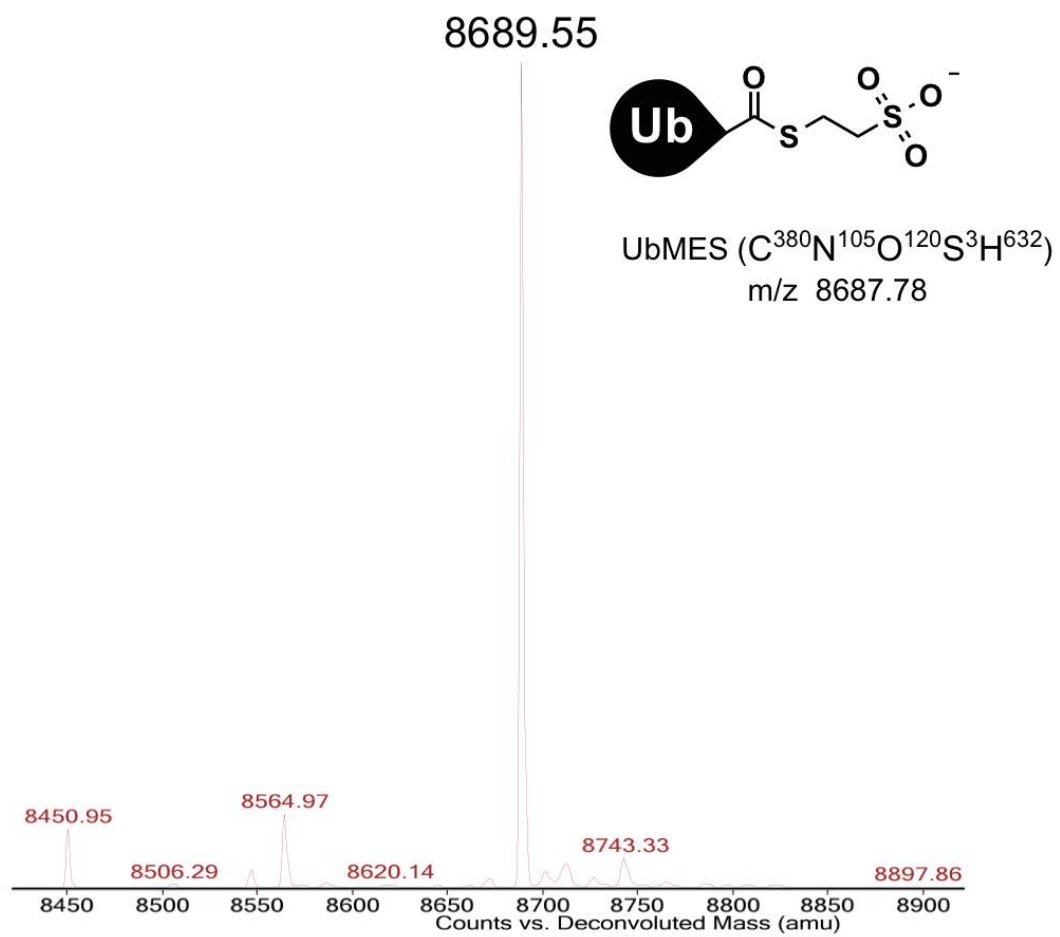
Supplementary Results



(B)



(C)



(D)

177 MGEEKEMKPACIKALT	191 RIFKISDQDN	201 DGTLNDAELN	211 FFQRICFNTP	221 LAPQALQEDVK
231 NVVRKHISDG	241 VADSGTLKLG	251 FLFLHTLFIQ	261 RGRHETTWTWV	271 LRRFGYDDDL
281 DLTPEYLFPL	291 LKIPPDCTTE	301 LNHHAYLFLQ	311 STFDKHDLDLDR	321 DCALSPDELK
331 DLFKVFPYIP	341 WGPDVNNTVC	351 TNERGWITYQ	361 GFLSQWTLTT	371 YLDVQRCLEY
381 LGYLGYSILT	391 EQESQASAVT	401 VTRDKKIDLQ	411 KKQTQRNVFR	421 CNVIGVKNCG
431 KSGVLQALLG	441 RNLMRQKKIR	451 EDHKSYAIN	461 TVVYVGQEKY	471 LLLHDISESE
481 FLTEAESFCD	491 VVCLVYDVSN	501 PNSLNTVARI	511 LSTTFMDSRI	521 TCLIRAAKSD
531 LHEVKQEYSI	541 SPTDFCRKHK	551 MPPPQAFTCN	561 TADAPSKDIF	571 VKLTTMAMYP
481 HVTQADLKSS	592 TFLEHHHHHHH			

(E)

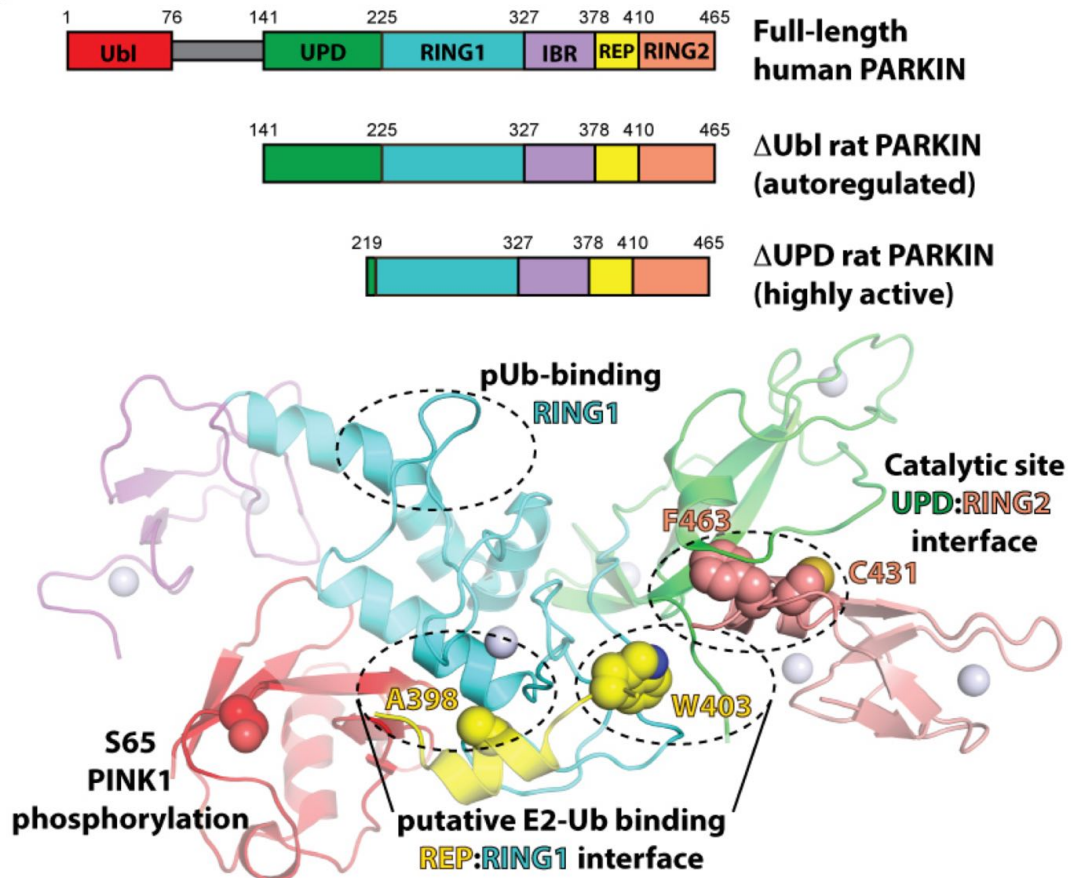
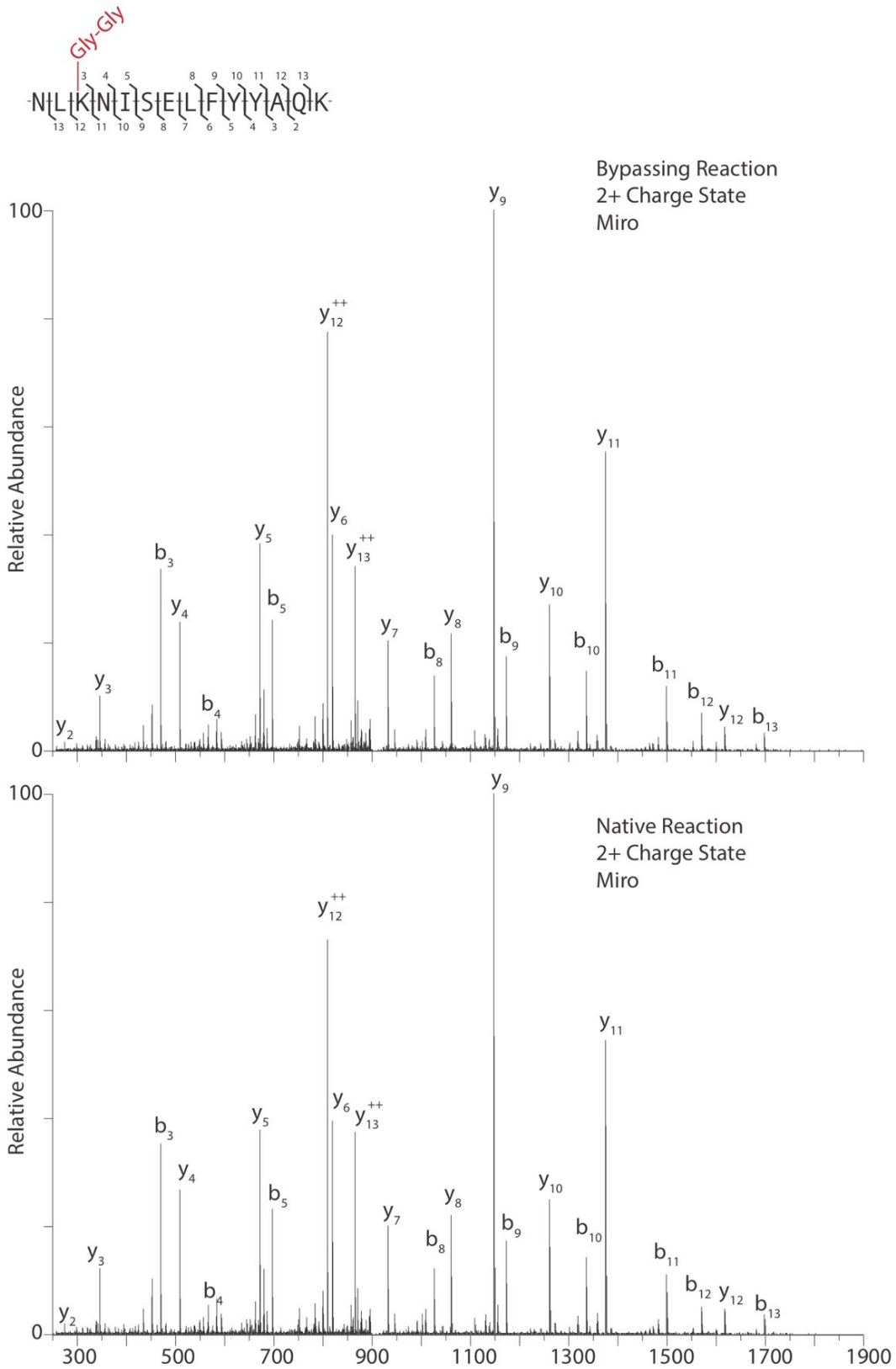
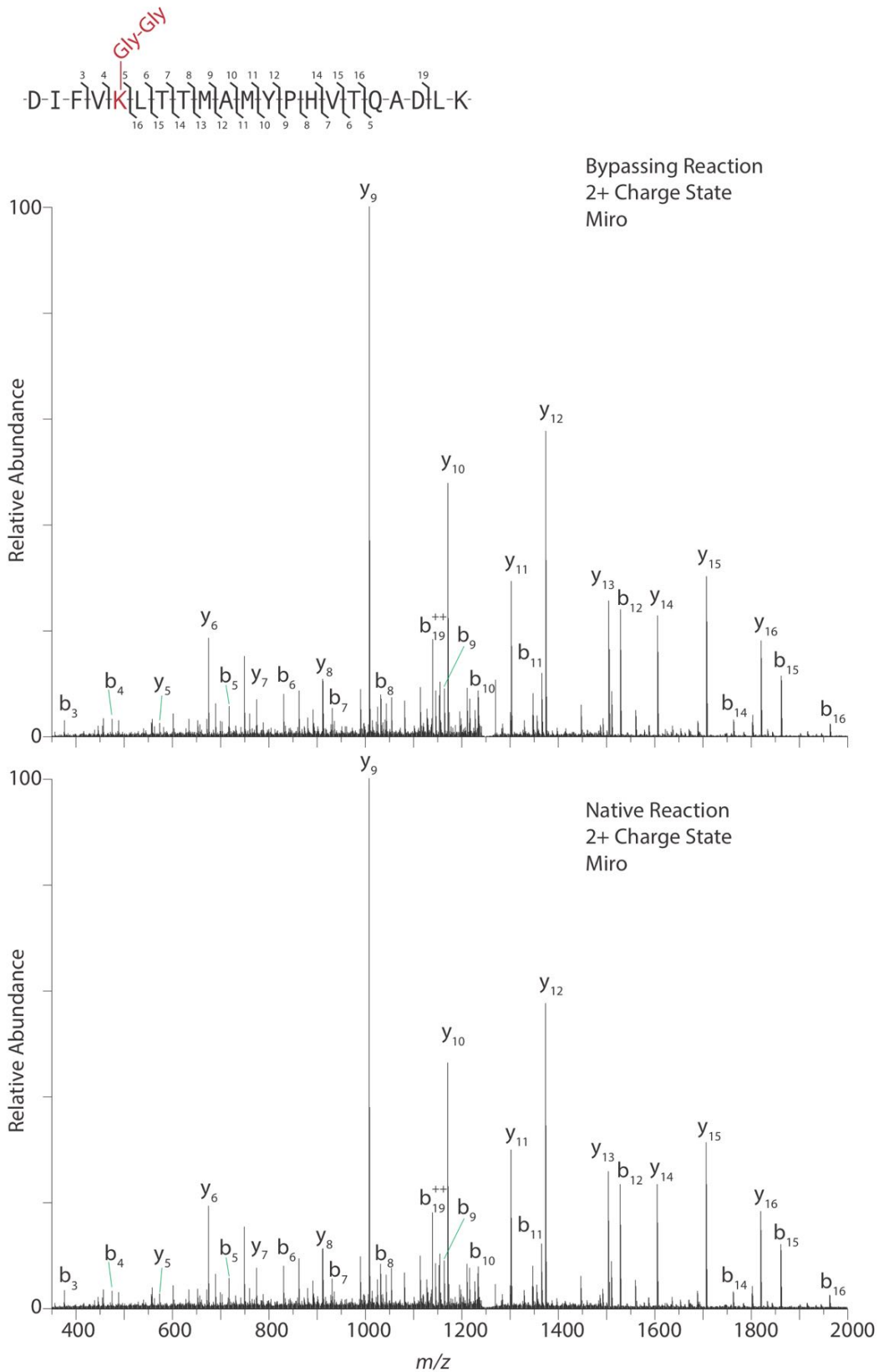


Figure S1. Preparation of the model system (A) pPARKIN migrates slower in a Phos-tag gel (Wako Industries, Richmond, VA), indicating phosphorylation, only when treated with TcPINK1 and ATP together. (B) Purified pPARKIN was digested by trypsin and analyzed for phosphorylation sites. We identified Ser⁶⁵ as well as nonspecific phosphorylation at Ser¹¹⁶ and Ser¹³¹ (C) Analysis of purified UbMES (described in Methods) using ESI-MS analysis. (D) Amino acid sequence of the PARKIN substrate MiroS used in this study, which is a truncated construct of Miro1 (177-592 with C-terminal 6xHis tag, 51.6 kDa). (E) Top, bar diagrams showing the PARKIN constructs used in this report. Bottom, structure of rat PARKIN structure (PDB ID #4K95)⁶ showing activating and inhibitory PARKIN mutations used in this study. Domains are colored as in the bar diagram above and as in the same report⁶. Mutated residues are shown in spacefill and zinc ions are shown as grey spheres. The putative pUb-binding region is based on the structure of pUb-PARKIN from a recent report⁷.

(A) Lys¹⁵³ of Miro1 is ubiquitinated



(B) Lys⁵⁷² of Miro1 is ubiquitinated



(C) Lys³³⁰ of Miro1 is ubiquitinated

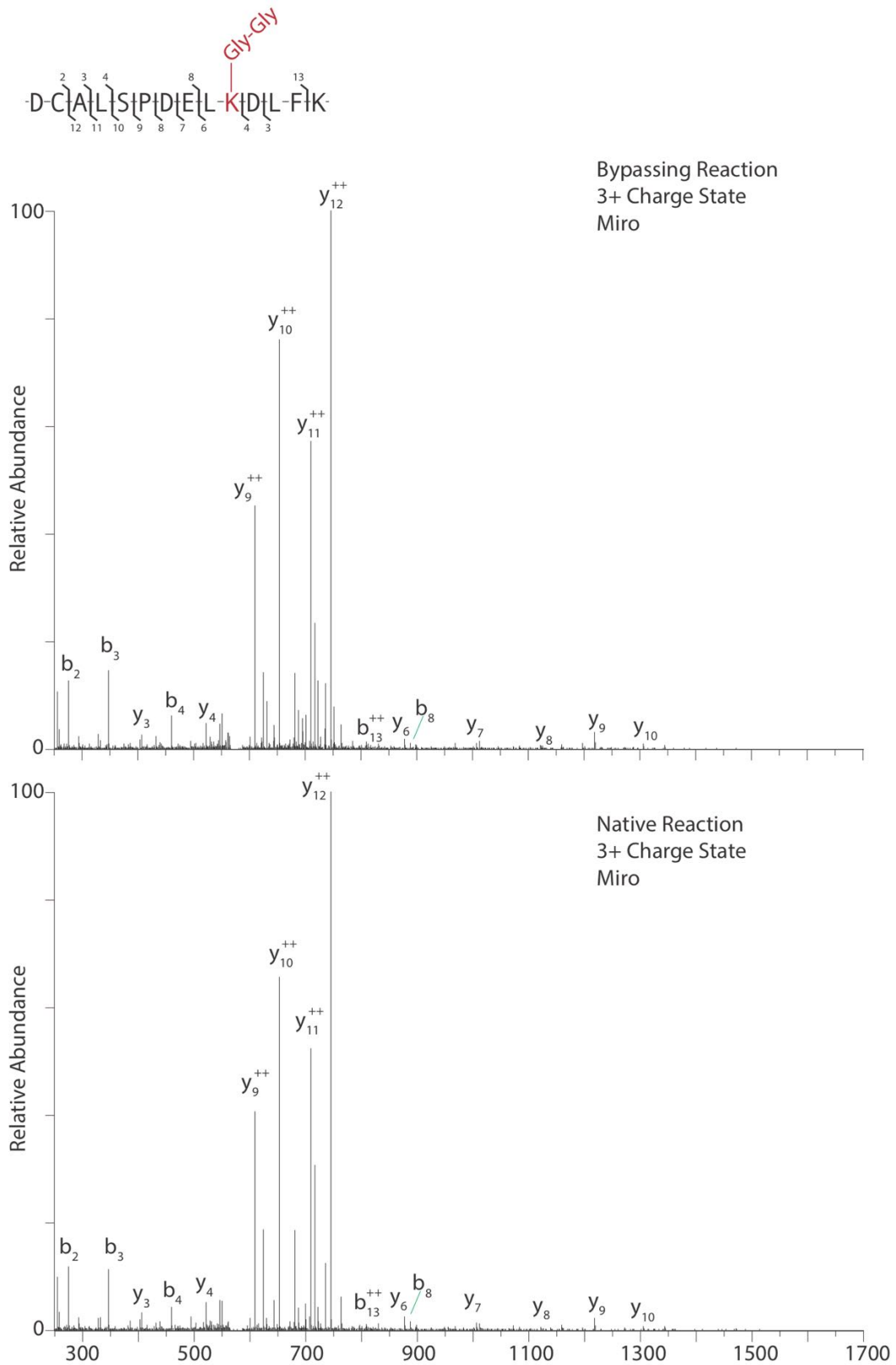


Figure S2. MS/MS analysis of Miro1 ubiquitination sites by pPARKIN under ByS and native reaction. Full length Miro1 was ubiquitinated minimally by using a small amount of ubiquitin in both ByS and native reactions. For the ByS reaction, 1 μ M MiroS, 5 μ M of UbMES and 1 μ M of pPARKIN were used. For the native reaction, 5 μ M of ubiquitin along with 0.1 μ M of E1, 1 μ M of Ubch7 and 1 μ M of pPARKIN were used. After 1 hour, the reactions were stopped, trypsinized and analyzed by MS/MS as described in the Methods section. The same lysines were ubiquitinated by pPARKIN under both reaction conditions: Lys¹⁵³ (A), Lys⁵⁷² (B) and Lys³³⁰ (C).

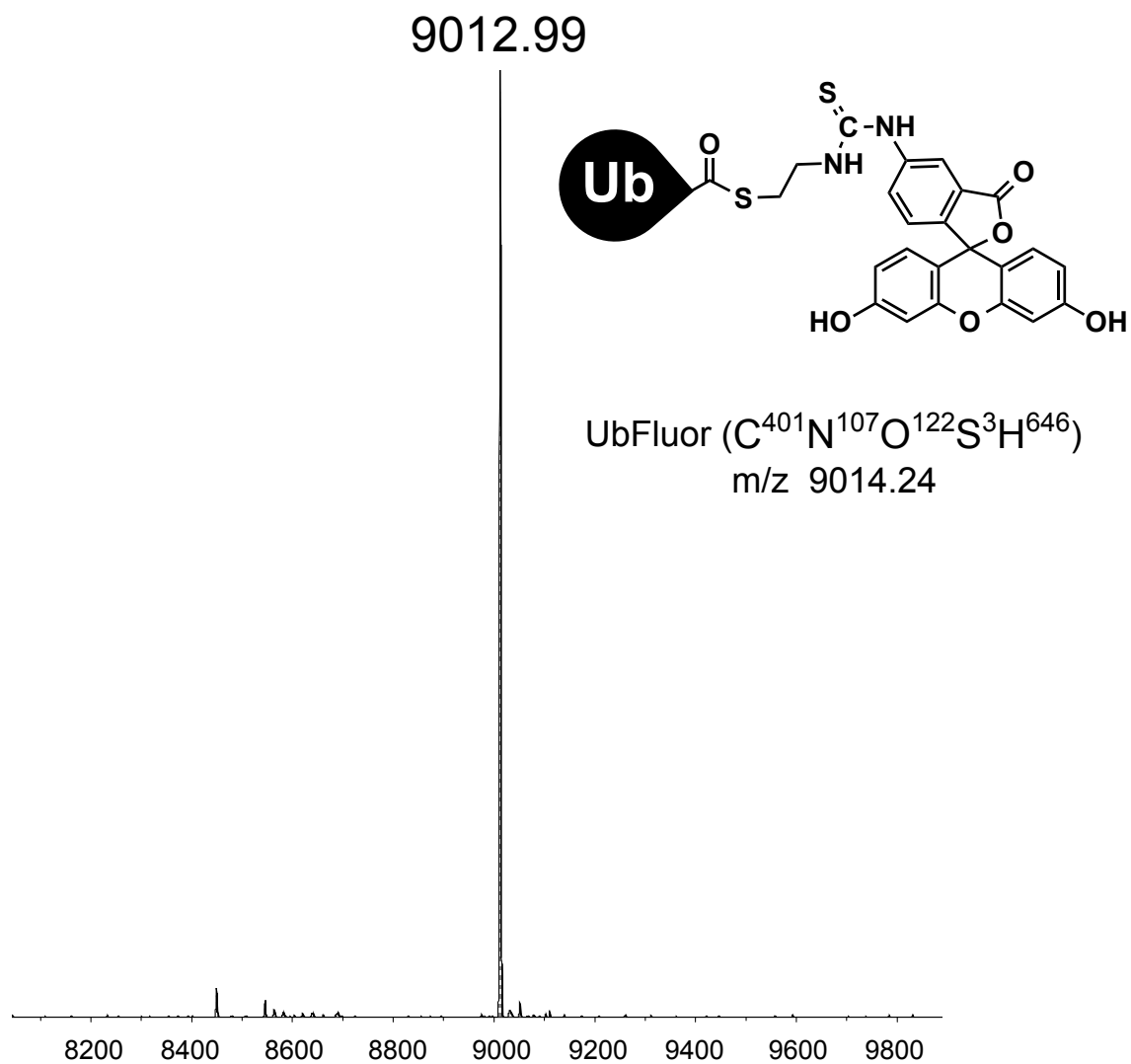


Figure S3. ESI-MS analysis of UbFluor Purified UbFluor was analyzed by ESI-MS analysis. The calculated mass of 9012.99 Da was the average molecular weight of the chemical formula.

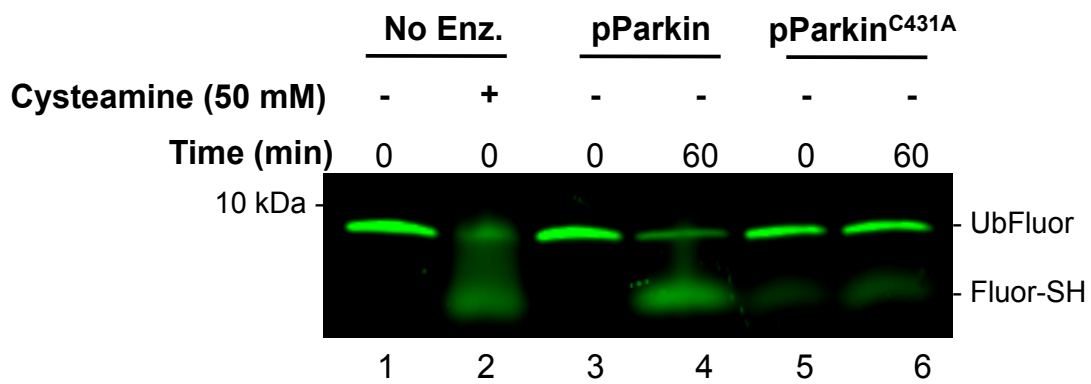
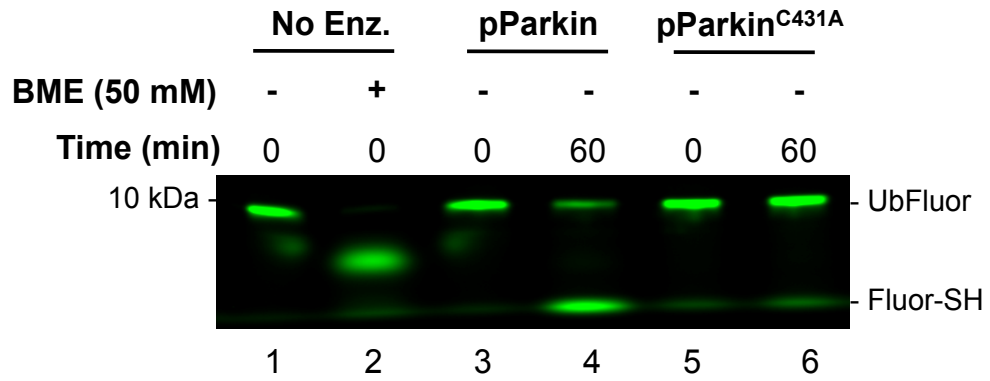


Figure S4. Cysteamine cleavage of UbFluor The experiment shown in Figure 3B was repeated using cysteamine in place of beta-mercaptoethanol (BME). Figure 3B shows that BME-released fluorescein thiol migrated slower than pPARKIN-released fluorescein thiol (Figure 3B, lane 2). This slower migration was not observed when cysteamine was used as a nucleophile, suggesting that the slow migration effect is BME-specific.

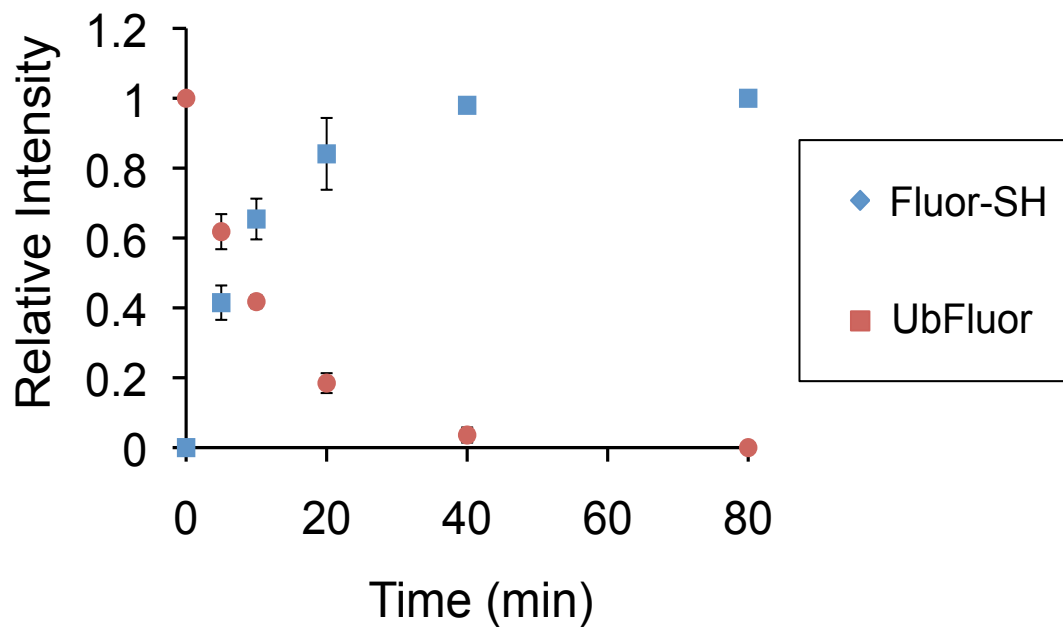
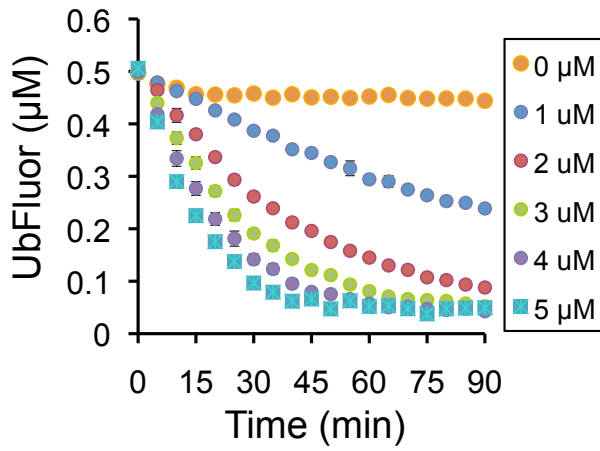
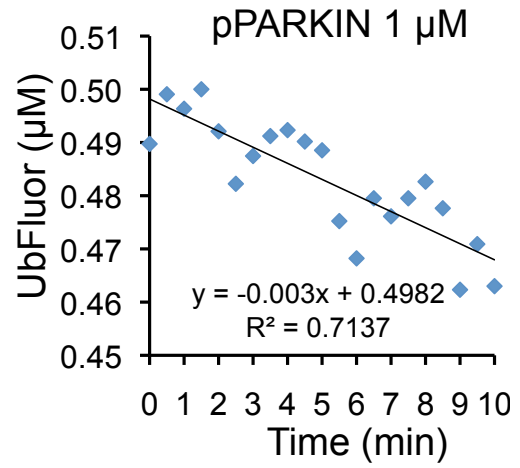


Figure S5. Fluorescence intensity quantification of Figure 3C. The UbFluor and free fluorescein thiol (Fluor-SH) band intensities at each time point were quantified using ImageJ and plotted vs. time. Error bars indicate standard error of the mean for 3 measurements.

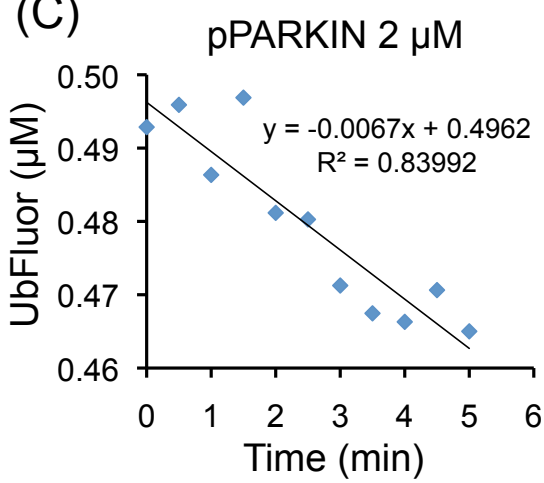
(A)



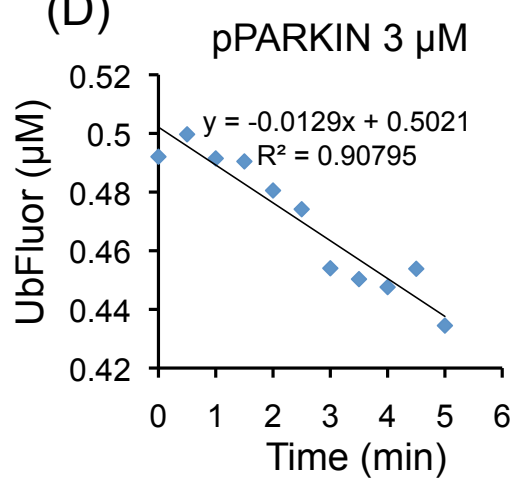
(B)



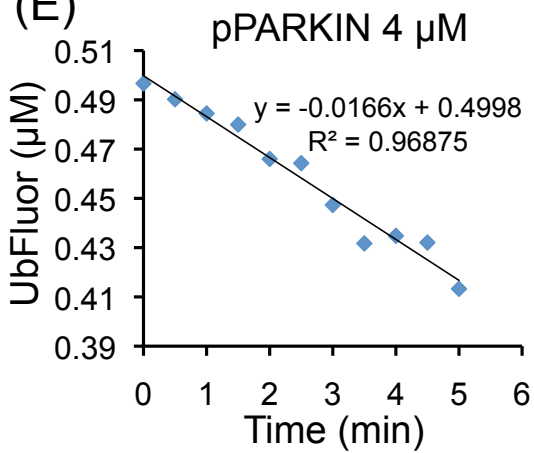
(C)



(D)



(E)



(F)

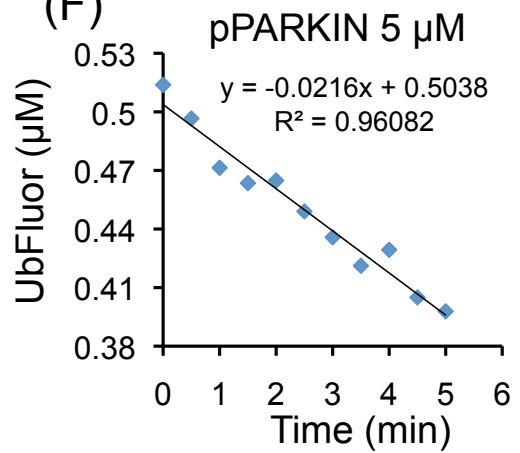


Figure S6. Data processing examples (A) The FP values shown in Figure 3 were converted to UbFluor concentrations as described in the methods section. 150 mP represents the starting UbFluor concentration of 0.5 μM while 30 mP represents complete consumption of UbFluor (0 μM). Standard errors of the mean for 3 separate measurements were determined, but are too small to see in the plot. The initial rates at 0 - 5 μM pPARKIN were determined as shown here. For 2, 3, 4 and 5 μM pPARKIN, a linear fit of the first 5 minutes of the reaction gave the initial rates. For 1 μM pPARKIN, the first 10 min were used due to the slower consumption of UbFluor. The data shown are representative of 3 replicate measurements. (B). These initial rates were plotted vs. pPARKIN concentration in Figure 3F.

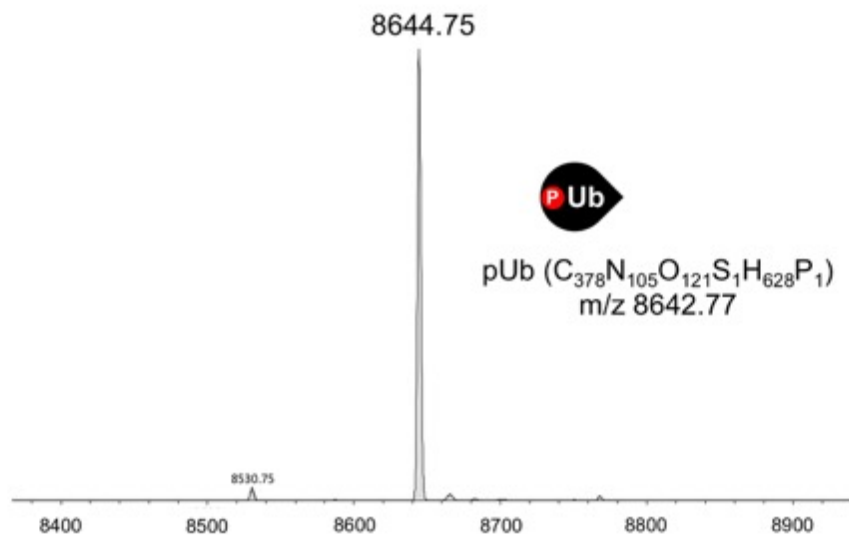


Figure S7. ESI-MS analysis of pUb Ubiquitin was phosphorylated using TcPINK1 and purified as described in Methods and analyzed by ESI-MS. The calculated mass of 8642.77 Da is the average molecular weight of the chemical formula.

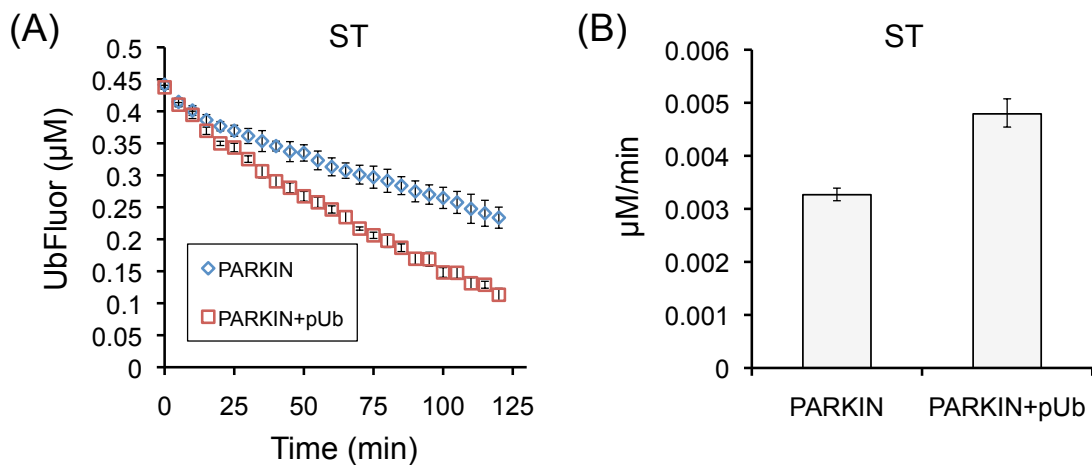


Figure S8. pUb moderately activates the catalytic site of PARKIN (A) UbFluor consumption was measured under ST conditions (5 μM PARKIN and 0.5 μM UbFluor) for PARKIN with or without 25 μM pUb. The activity difference between PARKIN and PARKIN + pUb becomes more obvious as reaction time is extended. Error bars indicate standard errors of the mean for three independent measurements. (B) The initial rate of UbFluor consumption was obtained for the two conditions as described in Figure S7. Error bars indicate standard errors of the mean for three replicate measurements.

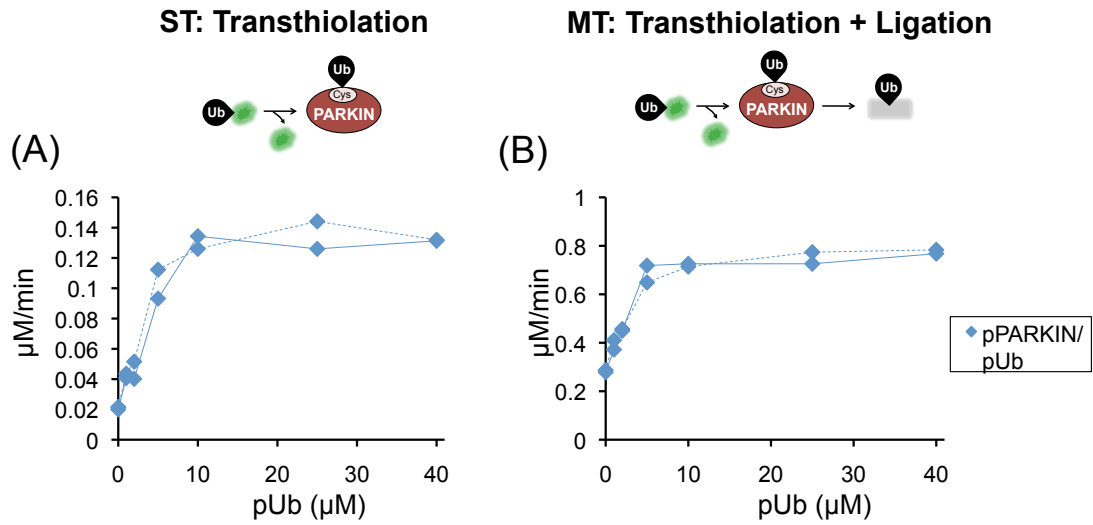


Figure S9. pUb titration to 40 μM . pPARKIN was titrated with pUb to 40 μM under ST (A) or MT (B) conditions. The maximal rates measured at 40 μM pUb are similar to the maximal rates obtained by addition of 25 μM pUb as shown in the text. Each titration was repeated twice and all data are shown. Solid lines join the rates determined from one titration experiment, while dashed lines join rates determined from a second titration.

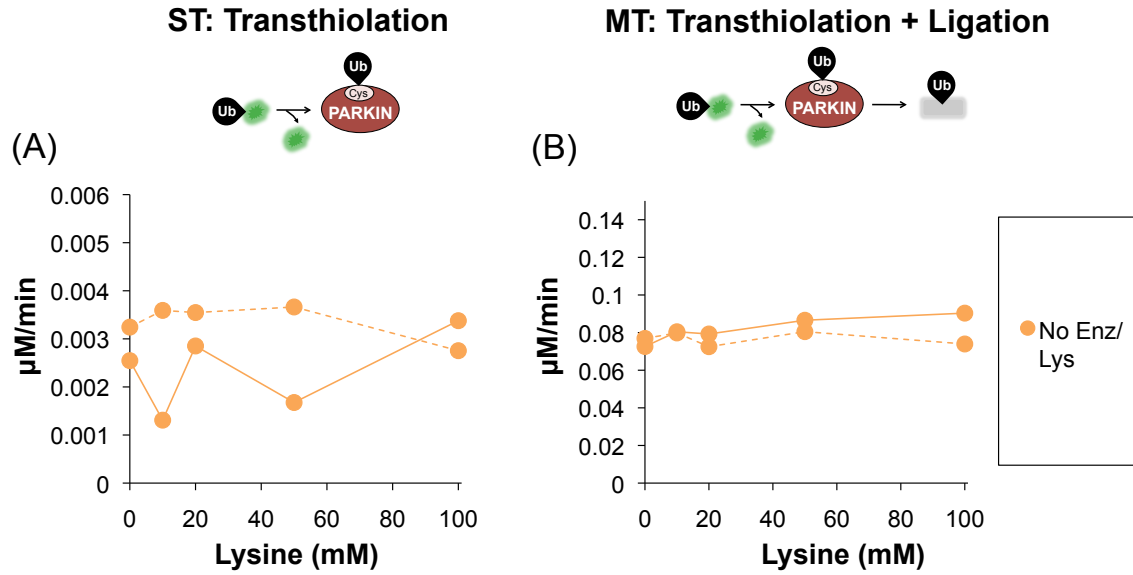


Figure S10. UbFluor is stable in the presence of up to 100 mM lysine. The figure shown is the same as Figure 4E-F with the consumption rate of UbFluor (y-axis) on a different scale to demonstrate stability of UbFluor. Lysine titrations were performed under both ST conditions (A); 0.5 μ M UbFluor, and MT conditions (B); 20 μ M UbFluor. Each titration was repeated twice and all data are shown. Solid lines join the rates determined from one titration experiment, while dashed lines join rates determined from the second titration.

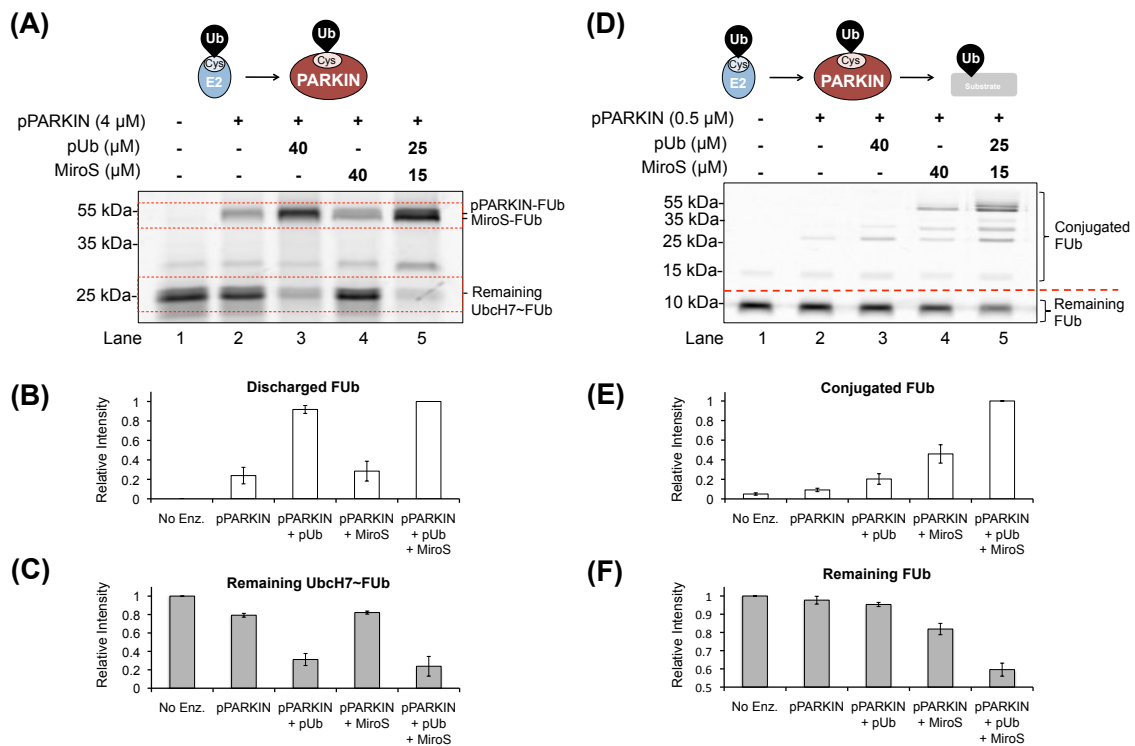
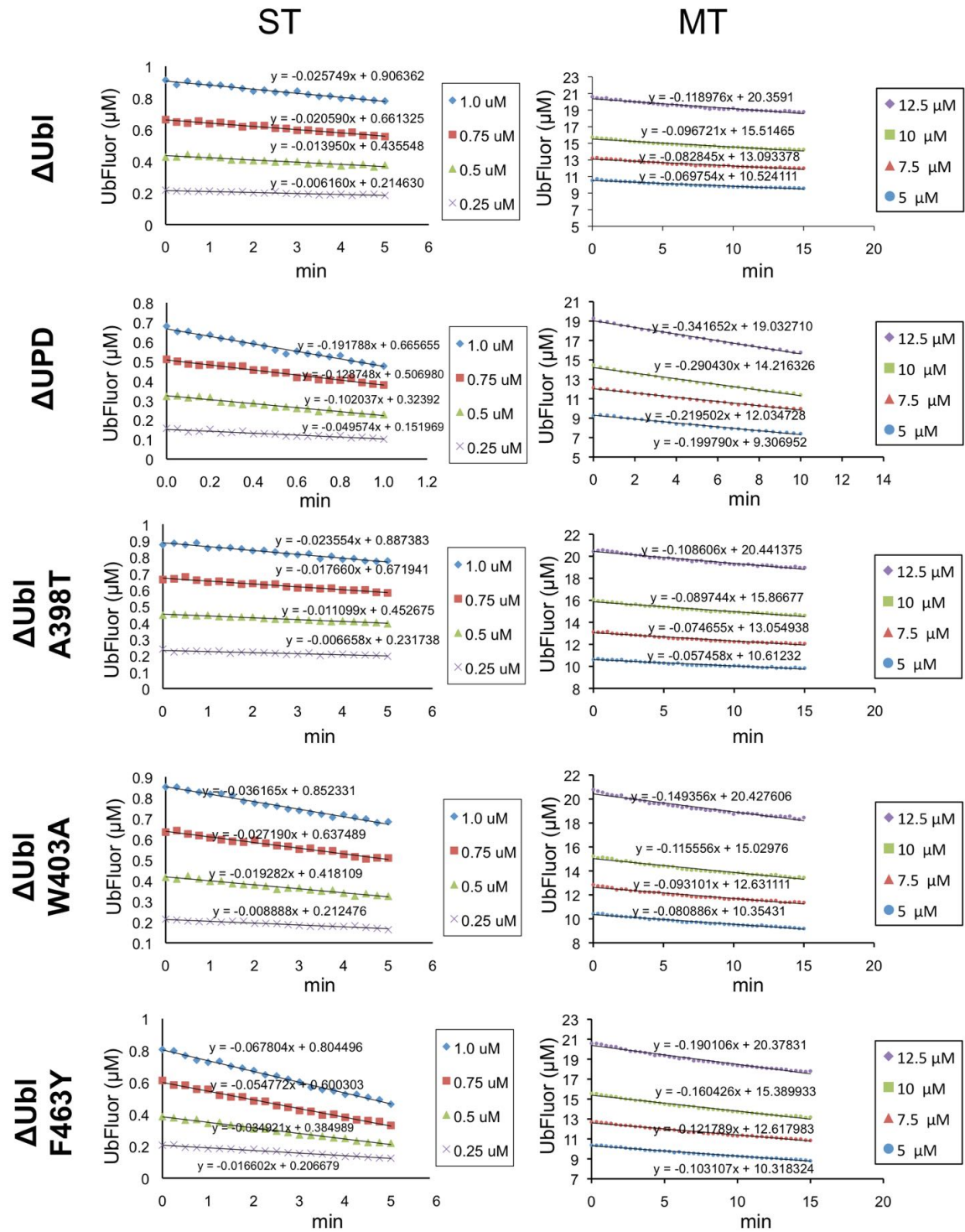


Figure S11. Comparison of MiroS and pUb for pPARKIN activation. The efficiency of pPARKIN for (A-C) Ubch7~FUb discharge, corresponding to transthiolation activity, and (D-F) total ubiquitin ligation turnover were analyzed by SDS-PAGE and fluorescent gel scanning. (A) The thioester conjugate of Ubch7 and fluorescent ubiquitin (Ubch7~FUb, 0.5 μ M, final) was prepared and chased as described in the methods section by adding chase buffer components and excess pPARKIN. Reactions were incubated on ice for 5 seconds before quenching with non-reducing Laemmli buffer. The fluorescence intensity of (B) upper, ~55 kDa bands (pPARKIN-FUb and MiroS-FUb) and (C) lower, ~25 kDa bands (remaining Ubch7~FUb) were quantified. (D) The E2~Ub charging reaction composed of E1 (0.5 μ M), Ubch7 (2 μ M) and FUb (15 μ M) was started by adding ATP (2 mM) for 20 minutes at room temperature. To the reaction, pPARKIN and indicated components were added. This was to minimize the effect of pUb~E2 formation that is inefficiently discharged by pPARKIN.⁸ The reaction was incubated for 1 minute at room temperature before quenching with reducing Laemmli buffer. The fluorescence intensity of (E) bands above 10 kDa (conjugated FUb) and (F) bands below 10 kDa (remaining FUb) were quantified. Error bars in both (C) and (F) indicate standard error of the mean for 3 measurements.

(A) Initial Rates



(B) Linear Least Squares Fitting

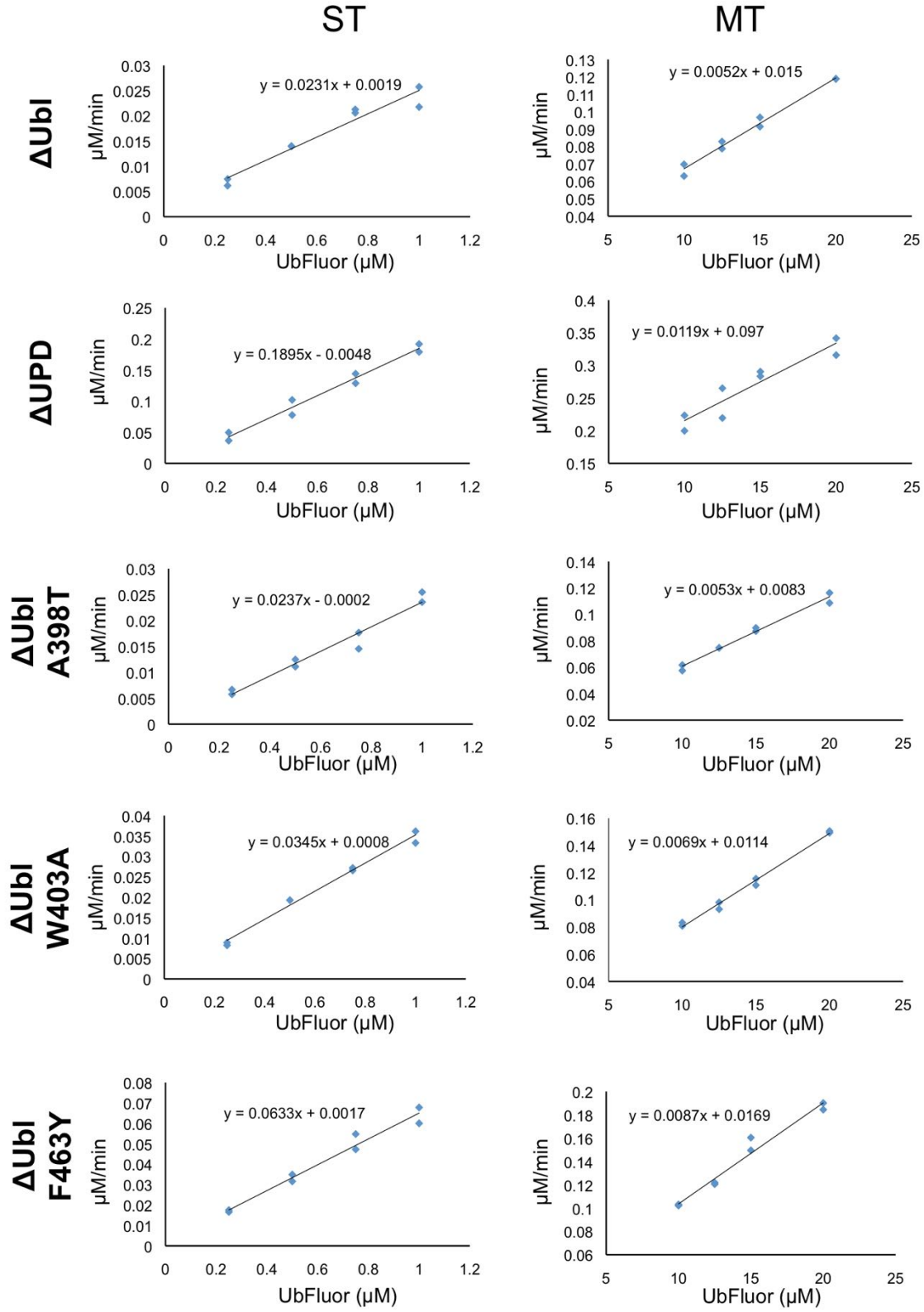


Figure S12. Data processing to obtain bimolecular rates (k_{obs}) for ΔUbl rat PARKIN constructs containing activating mutations. (A) For each construct, the initial rates were obtained at 4 different concentrations of UbFluor (0.25, 0.5, 0.75 and 1 μM of UbFluor for ST conditions or 5, 7.5, 10 and 12.5 μM UbFluor for MT conditions). For ST measurements, 5 μM of rat PARKIN was used while for MT measurements, 1 μM of rat PARKIN was used for all mutations except ΔUPD . For ΔUPD , 2 μM PARKIN was used for ST conditions because of its extremely fast reaction rate. For the same reason, the initial rate for ΔUPD was calculated using only data from 0 – 1.2 min for ΔUPD under ST conditions. Initial rates were determined using two datasets, and one dataset is shown in (A). (B) The initial rates from all 8 measurements were plotted vs. UbFluor concentration, and the data was fitted using a linear least squares (linest function, Microsoft Excel) to obtain the slope. The slope is divided by concentration of PARKIN to obtain k_{obs} ($\text{M}^{-1}\text{s}^{-1}$, Figure 6B). Reported errors in k_{obs} were determined from the error in the slope of the linear least squares fit.

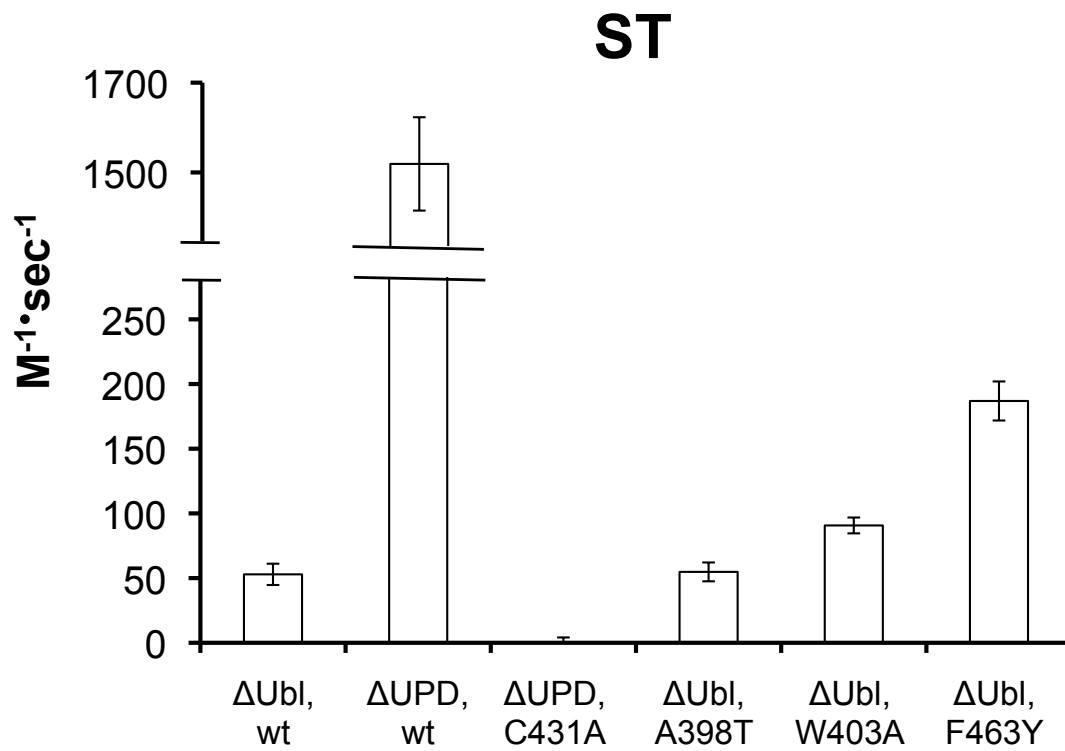
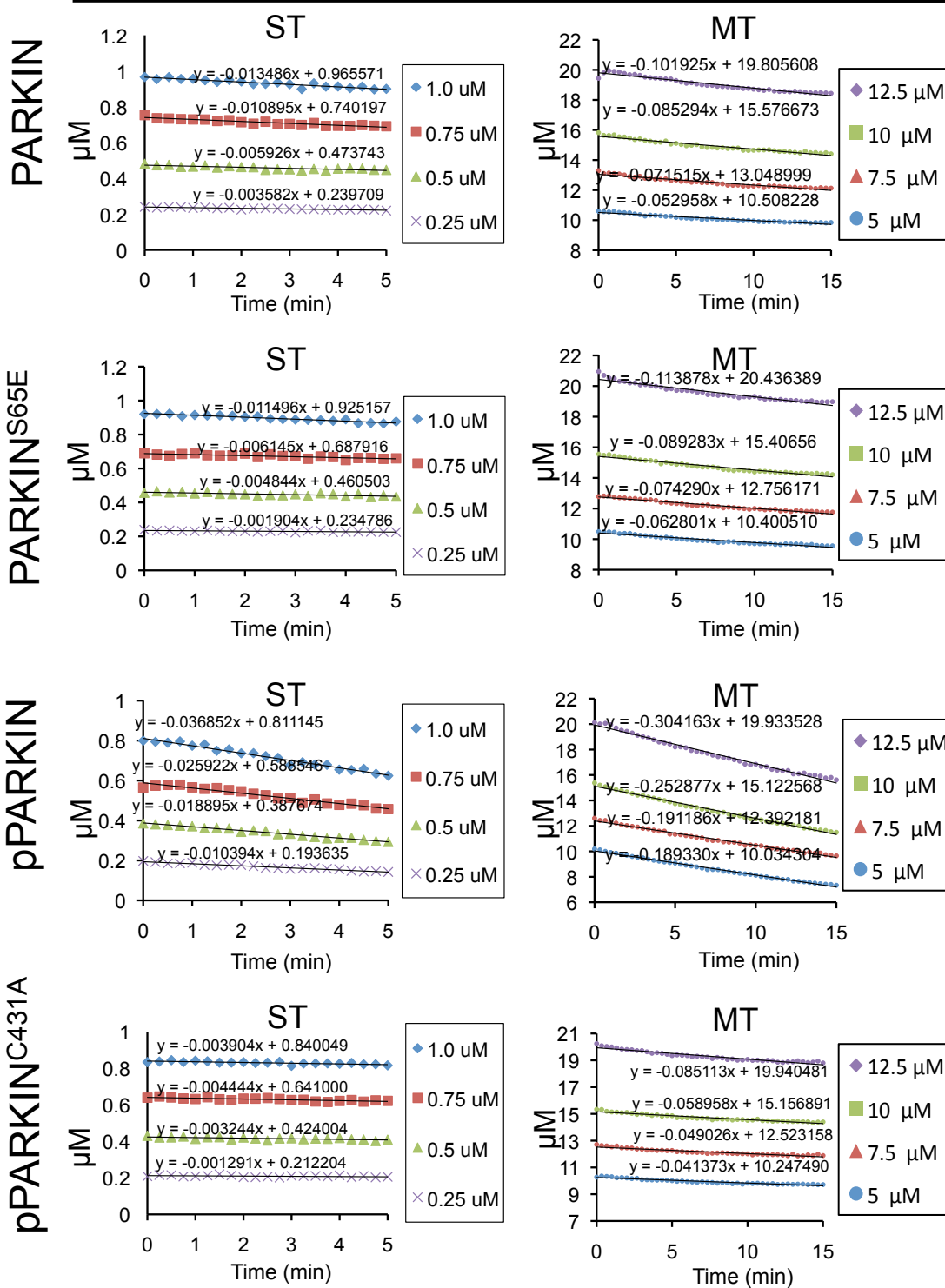
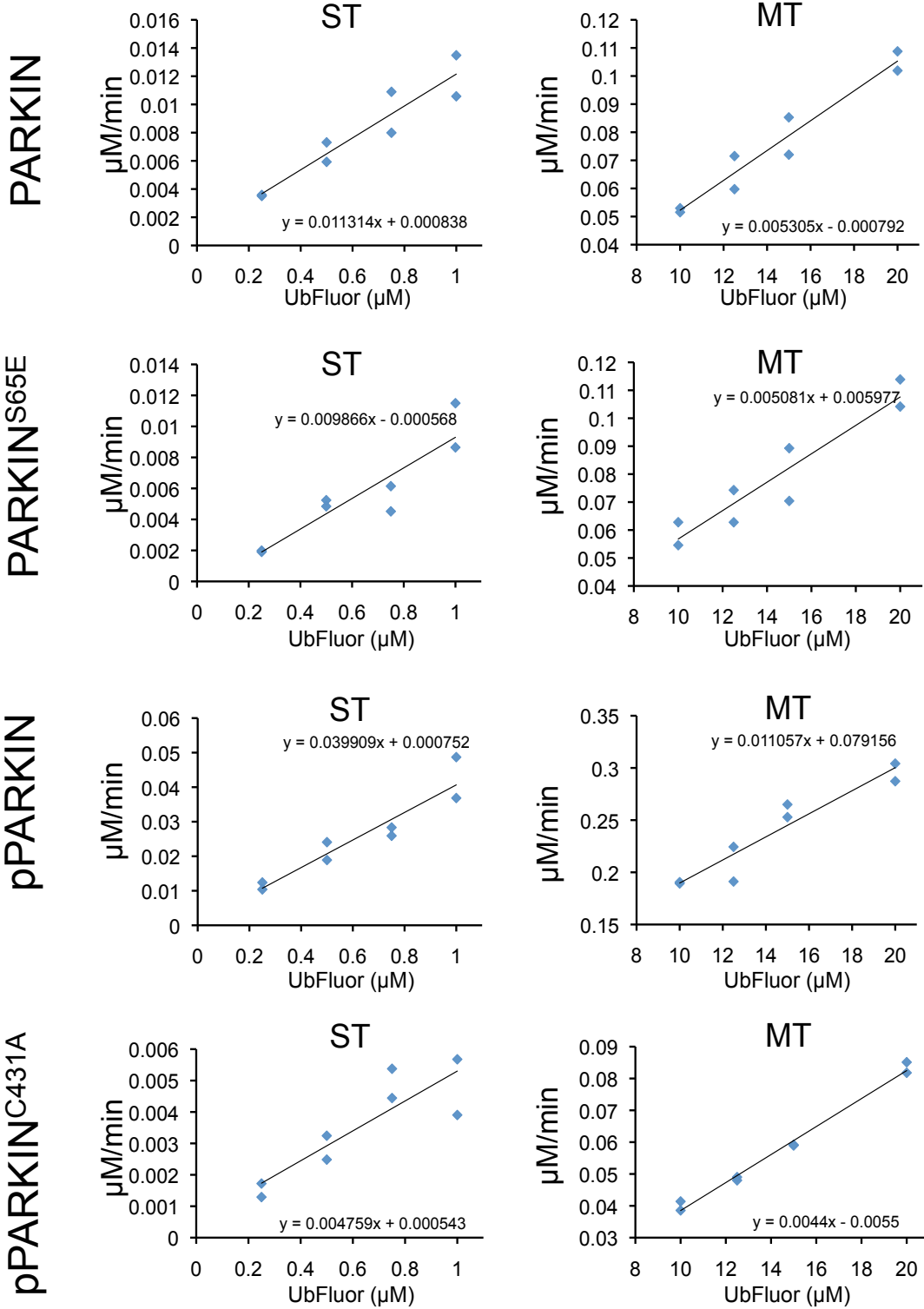


Figure S13. ST bimolecular rates for rat PARKIN constructs that are activated by known structural mutations. Along with activities of rat PARKIN mutants at MT conditions (Figure 6B), we obtained bimolecular rates under ST conditions as described in the text. Both ST and MT rates show similar trends.

(A) Initial Rates



(B) Linear Least Square Fitting



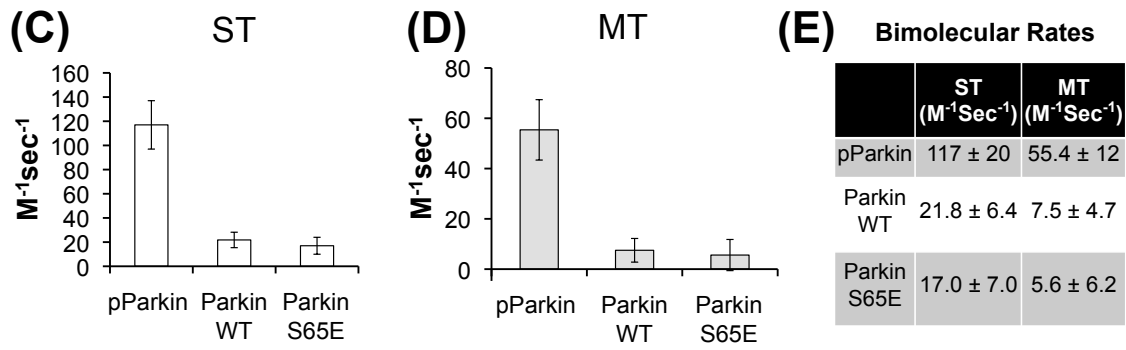


Figure S14. Data processing to obtain bimolecular rates (k_{obs}) for PARKIN^{S65E}. (A) The initial rates of each construct were obtained at 4 different concentrations of UbFluor as described in Figure S12. For ST measurements, 5 μ M of PARKIN was used while for MT measurements, 2 μ M of PARKIN was used. One of the two sets of data is shown. (B) The initial rates from all 8 measurements were plotted vs. UbFluor concentration and fitted using a linear least squares (linest function, Microsoft Excel) to obtain the slope. The slope was divided by the concentration of PARKIN to obtain k_{obs} (M⁻¹s⁻¹) (C-E). Reported errors in k_{obs} were determined from the error in the slope of the linear least squares fit.

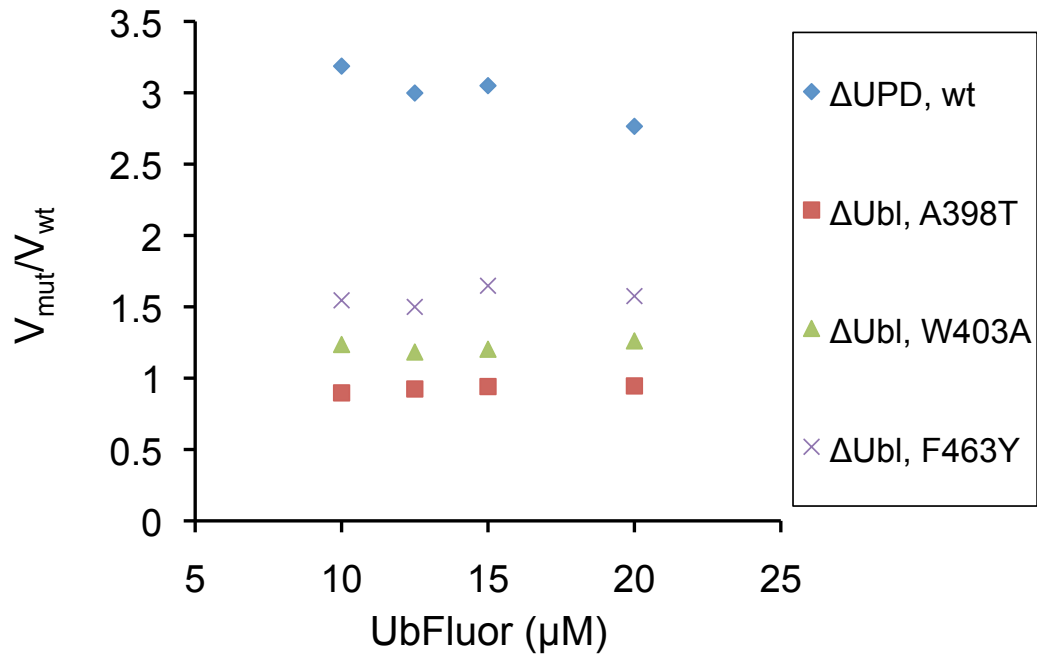
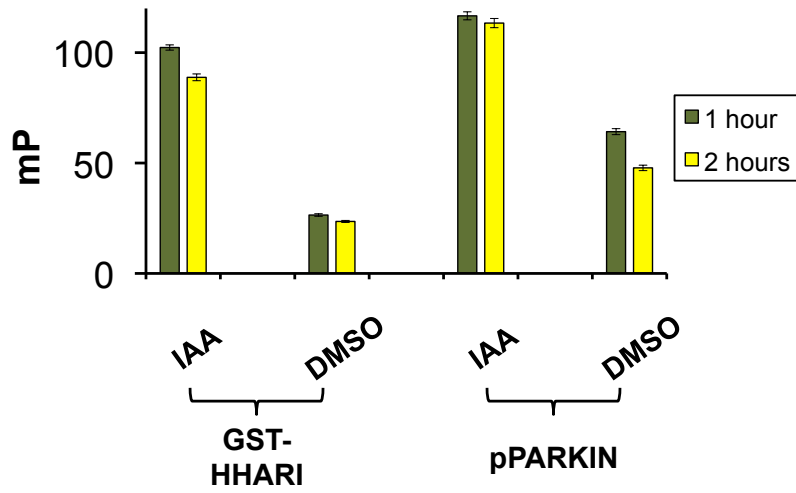


Figure S15. Bimolecular rates do not depend on UbFluor concentration in the range used for MT assays (10-20 μM UbFluor). To confirm that we can quantitatively assess and compare bimolecular rates for rat PARKIN mutants obtained at the 10 – 20 μM of UbFluor concentration used in this work, MT rates of each mutant obtained at each concentration of UbFluor were divided by the rates of the ΔUbl construct. The ratio of the mutant to wild-type rates (V_{mut}/V_{WT}) does not depend significantly on UbFluor concentration (<10% variation) in this range.

(A)



(B)

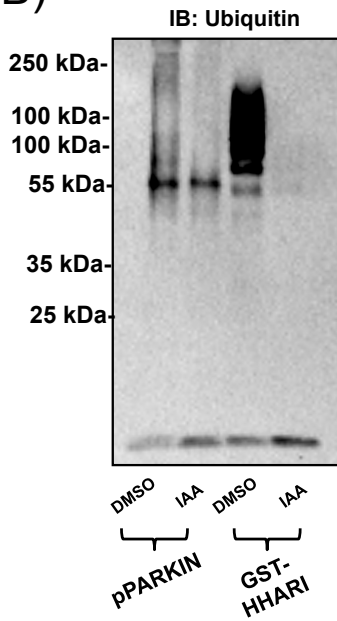


Figure S16. The UbFluor assay is suitable for high-throughput screening (A) The RBR E3 Ligases HHARI or PARKIN (1.0 μ M) were incubated in 50 mM HEPES pH 7.5, 50 mM NaCl, 0.5 mM TCEP, 6 μ M Tween-20 with either DMSO (0.2%) or with iodoacetamide (IAA, 1 mM in 0.2% DMSO) for 1 hour. UbFluor (5 μ M) was then added and incubated with the E3 ligase for 1 or 2 hours before endpoint fluorescence polarization readings were recorded with the Synergy 4 microplate reader (BioTek, Winooski, VT). Error bars indicate standard error of the mean for 3 measurements. (B) The same reactions were quenched with reducing Laemmli buffer, resolved with SDS-PAGE and Western blotted using an anti-Ub antibody.

SI References

1. S. Baumann, S. Schoof, M. Bolten, C. Haering, M. Takagi, K. Shin-ya and H. D. Arndt, *J Am Chem Soc*, 2010, **132**, 6973-6981.
2. F. El Oualid, R. Merkx, R. Ekkebus, D. S. Hameed, J. J. Smit, A. de Jong, H. Hilkmann, T. K. Sixma and H. Ovaa, *Angewandte Chemie*, 2010, **49**, 10149-10153.
3. A. Kazlauskaitė, C. Kondapalli, R. Gourlay, D. G. Campbell, M. S. Ritorto, K. Hofmann, D. R. Alessi, A. Knebel, M. Trost and M. M. K. Muqit, *Biochem J*, 2014, **460**, 127-139.
4. J. Mikolajczyk, M. Drag, M. Bekes, J. T. Cao, Z. Ronai and G. S. Salvesen, *J Biol Chem*, 2007, **282**, 26217-26224.
5. A. Ordureau, S. A. Sarraf, D. M. Duda, J. M. Heo, M. P. Jedrychowski, V. O. Sviderskiy, J. L. Olszewski, J. T. Koerber, T. Xie, S. A. Beausoleil, J. A. Wells, S. P. Gygi, B. A. Schulman and J. W. Harper, *Molecular cell*, 2014, **56**, 360-375.
6. J. F. Trempe, V. Sauve, K. Grenier, M. Seirafi, M. Y. Tang, M. Menade, S. Al-Abdul-Wahid, J. Krett, K. Wong, G. Kozlov, B. Nagar, E. A. Fon and K. Gehring, *Science*, 2013, **340**, 1451-1455.
7. T. Wauer, M. Simicek, A. Schubert and D. Komander, *Nature*, 2015, DOI: 10.1038/nature14879.
8. T. Wauer, K. N. Swatek, J. L. Wagstaff, C. Gladkova, J. N. Pruneda, M. A. Michel, M. Gersch, C. M. Johnson, S. M. Freund and D. Komander, *Embo J*, 2014, DOI: 10.15252/emj.201489847.